PROCEEDINGS OF SCIENCE

# Lattice QCD Determination of the Bjorken-$x$ Dependence of PDFs at NNLO

**Xiang Gao,**[a,*] **Andrew D. Hanlon,**[b] **Swagato Mukherjee,**[b] **Peter Petreczky,**[b] **Philipp Scior,**[b] **Sergey Syritsyn**[c,d] **and Yong Zhao**[a]

[a] *Physics Division, Argonne National Laboratory, Lemont, IL 60439, USA*
[b] *Physics Department, Brookhaven National Laboratory, Bldg. 510A, Upton, New York 11973, USA*
[c] *RIKEN-BNL Research Center, Brookhaven National Laboratory, Upton, New York 11973*
[d] *Department of Physics and Astronomy, Stony Brook University, Stony Brook, New York 11790*

*E-mail:* gaox@anl.gov

We present lattice QCD calculation of pion valence quark distribution using next-to-next-to-leading order perturbative matching. We use three lattices with fine lattice spacings of $a$ = 0.04, 0.06 and 0.076 fm and two valence pion mass $m_\pi$=300 MeV and 140 MeV to have both discretization and pion mass effect under control. The bare quasi-PDF matrix elements of pion extracted from three-point functions are renormalized in the hybrid scheme and matched to the $\overline{\text{MS}}$ scheme. With boost momentum as large as 2.42 GeV, we present reliable lattice QCD prediction of Bjorken-$x$ dependent valence quark distribution of pion in middle $x$ region with controlled systematics.

*The 39th International Symposium on Lattice Field Theory,*
*8th-13th August, 2022,*
*Rheinische Friedrich-Wilhelms-Universität Bonn, Bonn, Germany*

*Speaker





PoS(LATTICE2022)104

## 1. Introduction

Parton distribution functions, which describe the momentum fraction $x$ of parent hadron carried by the parton, are universal quantities that can be extract from many kinds of high-energy scattering experiments [1, 2]. They have attracted great interest for decades because, on the one hand they are related to the hadron structure and tomography which can tell us how hadrons are built of fundamental degree of freedom of strong interaction [3]. On the other hand, they are critical input for the high-energy phenomenology as standard model backgrounds. However due to the confinement nature of strong interactions, the PDFs of hadron are the non-perturbative quantities so that can only be extracted from the experimental cross-sections or calculated by non-perturbative techniques. With decades' effort, the unpolarized PDF of nucleon has been determined with very good precision through the global analysis of experimental data, but the other kinds of PDFs still have large uncertainties. Due to the lack of fixed targets, the PDFs of pion, which is the Nambu-Goldstone bosons of QCD, are less constrained. Therefore any compensatory information provided by lattice QCD calculations will be essential.

As light-like quantities, the matrix elements of PDFs can't be directly computed from Euclidean lattice QCD for a long time. Until less than a decade ago, it was proposed to calculate the matrix elements of equal-time operators using highly boosted hadron states, namely the large momentum effective theory (LaMET) [4–6]. The quasi-PDFs defined as the Fourier transform of renormalized equal-time matrix elements differs from PDFs only in the ultraviolet (UV) region which can be corrected through perturbation theory. Much progress has been made in past few years for the calculation of PDFs of nucleon [6–12] and pion [13–25]. In this work, we focus on the valence quark distribution of pion. We will use the most advanced hybrid scheme to renormalize the bare matrix elements calculated from three different lattices and the next-to-next-leading-order (NNLO) factorization coefficients for the perturbative matching. Many systematics will be discussed to present reliable prediction of $x$ dependent pion valence quark distribution with control uncertainties.

## 2. Lattice calculation

The bare quasi-PDF matrix elements $\tilde{h}(z, P^z, a) \equiv \langle P|O_{\gamma^t}(z)|P\rangle/(2P^t)$ can be extracted from the analysis of two-point and three-point functions,

$$\begin{aligned} C_{2\text{pt}}(t_s; P_z) &= \left\langle \pi_S(\mathbf{x_0}, t_s)\pi_S^\dagger(\mathbf{P}, 0)\right\rangle, \\ C_{3\text{pt}}(z, \tau, t_s) &= \left\langle \pi_S(\mathbf{x_0}, t_s)O_\Gamma(z, \tau)\pi_S^\dagger(\mathbf{P}, 0)\right\rangle, \end{aligned} \tag{1}$$

where $\pi_S(\mathbf{x_0}, t_s)$ is the pion source after boosted smearing. The iso-vector operator $O_\Gamma(z, \tau)$ inserted at time slice $\tau$ is defined as

$$O_\Gamma(z, \tau) = \sum_{\mathbf{x}} \left[\overline{u}(x + \mathcal{L})\Gamma W_z(x + \mathcal{L}, x)u(x) - \overline{d}(x + \mathcal{L})\Gamma W_z(x + \mathcal{L}, x)d(x)\right], \tag{2}$$

with $x = (\mathbf{x}, \tau)$ and $\Gamma = \gamma_0$ as considered in this work.

In this work, we use three gauge ensembles with fine lattice spacings $a = 0.04$, 0.06 and 0.76 fm in 2+1 flavor QCD generated by the HotQCD collaboration [26] with Highly Improved Staggered

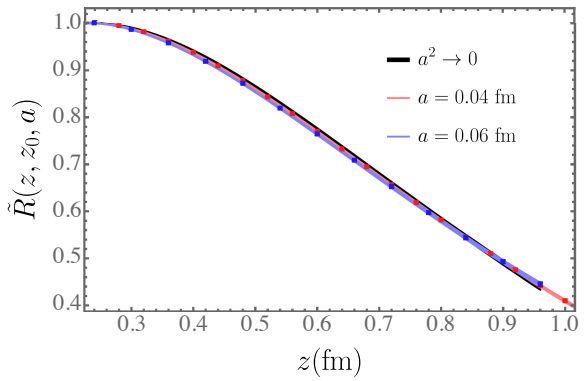


**Figure 1:** The ratio $\tilde{h}^{\rm lat}(z, P^z, z_S)$ with $z_S = 0.24$ fm of $P_z = 0$ case. The red and blue points are for $a = 0.04$ fm and 0.06 fm. The red and blue bands are interpolations of the points, and the gray band is the continuum extrapolation of them with $a^2$-dependence.

Quarks [27]. We use the Wilson-Clover action in the valence sector with valence pion mass tuned to be 300 MeV for the two finer lattice and 140 MeV for the coarser lattice. Furthermore, the Wilson lines in $O_\Gamma(z)$ were applied 1-step HYP smearing. We use pion momenta $P^z = (2\pi n_z)/(L_s a)$ with $0 \le n_z \le n_{\rm max}$, resulting in $P^z$ as large as 2.42 GeV for 300 MeV pion and 1.78 GeV for 140 MeV pion.

## 3. Renormalization and matching

The bare matrix matrix elements need to be renormalized. It is known that the operator $O_\Gamma(z)$ can be renormalized multiplicatively [28–30]

$$O^B_\Gamma(z, a) = e^{-\delta m(a)|z|} Z_O(a) O^R_\Gamma(z)\,, \tag{3}$$

where the logarithmic ultraviolet (UV) divergences are included in $Z_O(a)$, and the linear UV divergence $\propto 1/a$ originating from Wilson-line self energy as well as the renormalon ambiguity [31] are included in $\delta m(a)$,

$$\delta m(a) = \frac{m_{-1}(a)}{a} + m_0. \tag{4}$$

We utilize the hybrid scheme to remove the UV divergences in this work [32]: in the short distance $z_S \ll 1/\Lambda_{\rm QCD}$ we construct the RG invariant ratio scheme $\tilde{h}(z, P^z, a)/\tilde{h}(z, 0, a)$, while in the long distance $z_S > 1/\Lambda_{\rm QCD}$ we fix the denominator as $\tilde{h}(z_S, 0, a)$ to cancel the $Z_O(a)$ and furtherly remove the linear divergence by the Wilson-line mass $\delta m(a)$ estimated from the static quark-antiquark potential, namely,

$$\tilde{h}^{\rm lat}(z, P^z, z_S) = e^{\delta m(a)(z - z_S)} \frac{\tilde{h}(z, P^z, a)}{\tilde{h}(z_S, 0, a)} \tag{5}$$

In this work, we choose $z_S = 0.24$ fm. We show the $\tilde{h}^{\rm lat}(z, P^z, z_S)$ of $P_z = 0$ case in Fig. 1, where good continuum condition can be observed.

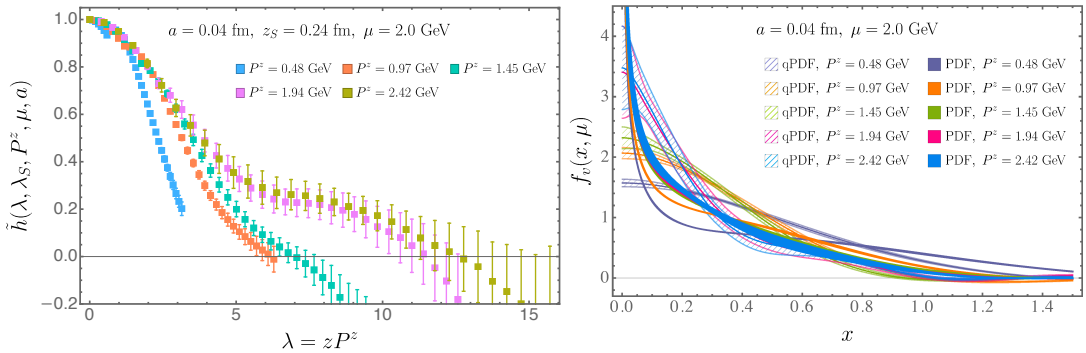


**Figure 2:** Left: Renormalized matrix elements in the hybrid scheme. Right: the corresponding qPDFs and PDFs after NNLO matching.

Since the renormalon ambiguity $m_0$ is scheme dependent, the lattice scheme $\tilde{h}^{\rm lat}(z, P^z, z_S)$ need to be matched to the $\overline{\rm MS}$ scheme to be consistent with our perturbative matching formula, which can be done by comparing with $\overline{\rm MS}$ operator product expansion (OPE) [33],

$$\lim_{a\to 0} \tilde{h}^{\rm lat}(z, P^z = 0, z_S) = e^{-\bar{m}_0(z-z_S)} \frac{C_0(\mu^2 z^2) + \Lambda z^2}{C_0(\mu^2 z_S^2) + \Lambda z_S^2}\,, \tag{6}$$

The Wilson coefficients $C_0$ are known to NNLO [34–36] from perturbation theory, and $\bar{m}_0 = -m_0^{\rm lat} + m_0^{\overline{\rm MS}}$ as well as $\Lambda z^2$ originated from the leading UV and infrared renormalons in $C_0$ [37]. With fixed order $C_0$, both $\bar{m}_0$ and $\Lambda$ depend on $\mu$ so do to the the $\overline{\rm MS}$ matrix elements,

$$\tilde{h}(z, z_S, P^z, \mu) = \frac{\tilde{h}(z, P^z, a)}{\tilde{h}(z, 0, a)}\theta(z_S - z) + e^{\delta m'(z-z_S)} \frac{\tilde{h}(z, P^z, a)}{\tilde{h}(z_S, 0, a)}\theta(z - z_S)\,, \tag{7}$$

where $\delta m' = \delta m + \bar{m}_0$ and in practice we normalize the matrix elements by dividing $N = \tilde{h}(0, P^z, a)/\tilde{h}(0, 0, a)$ and also correct the LO infrared renormalons in denominators. The renormalized matrix elements of several momentum are shown in the left panel of Fig. 2, while the corresponding quasi-PDF (qPDF) $\tilde{f}_v(x, P^z, \mu) = \int \frac{dz}{2\pi} e^{ixP^z z}\, \tilde{h}(z, z_S, P^z, \mu)$ are shown in the right panel. Based on LaMET [32, 34, 38, 39] factorization, we will be able to calculate the PDF $f_v(x, \mu)$ with $P^z$-controlled power corrections as,

$$f_v(x, \mu) = \int_{-\infty}^{\infty} \frac{dy}{|y|}\, C^{-1}\left(\frac{x}{y}, \frac{\mu}{yP^z}, |y|\lambda_S\right) \tilde{f}_v(y, \lambda_S, P^z, \mu) + O\left(\frac{\Lambda_{\rm QCD}^2}{(xP^z)^2}, \frac{\Lambda_{\rm QCD}^2}{((1-x)P^z)^2}\right), \tag{8}$$

with $\lambda_S = z_S P^z$ and $z_S = 0.24$ fm. Here $C^{-1}$ [33] is the inverse of the hybrid-scheme matching coefficient $C$ currently up to NNLO accuracy [35, 36]. The PDF after NNLO correction at scale $\mu = 2$ GeV are shown in the right panel of Fig. 2 labeled as PDF. Due to the power corrections, we will be able to control the middle region of $x \in [x_{\rm min}, x_{\rm max}]$.

## 4. Systematics and results

To present reliable prediction of $x$ dependent PDFs from lattice calculation, we need to control the possible systematics in addition to the statistical errors, including the lattice artifacts, perturbative

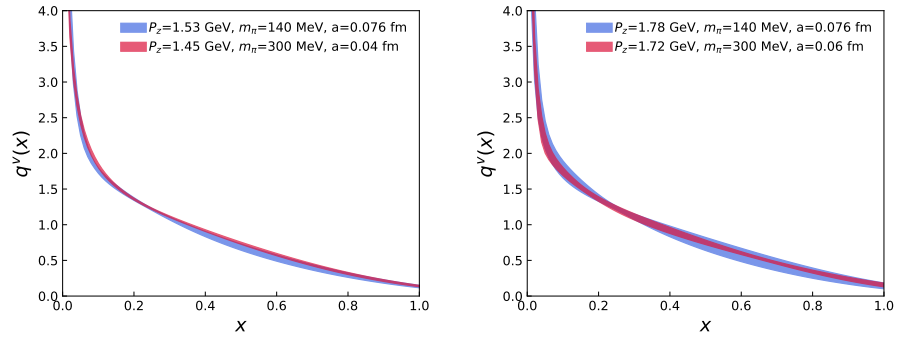


**Figure 3:** The valence quark distribution $f_v(x,\mu)s$ of pion obtained from the LaMET matching at NNLO level are shown. We compare the results from the $m_\pi$ = 140 MeV case (blue bands) and the $m_\pi$ = 300 MeV cases (red bands) for comparison.

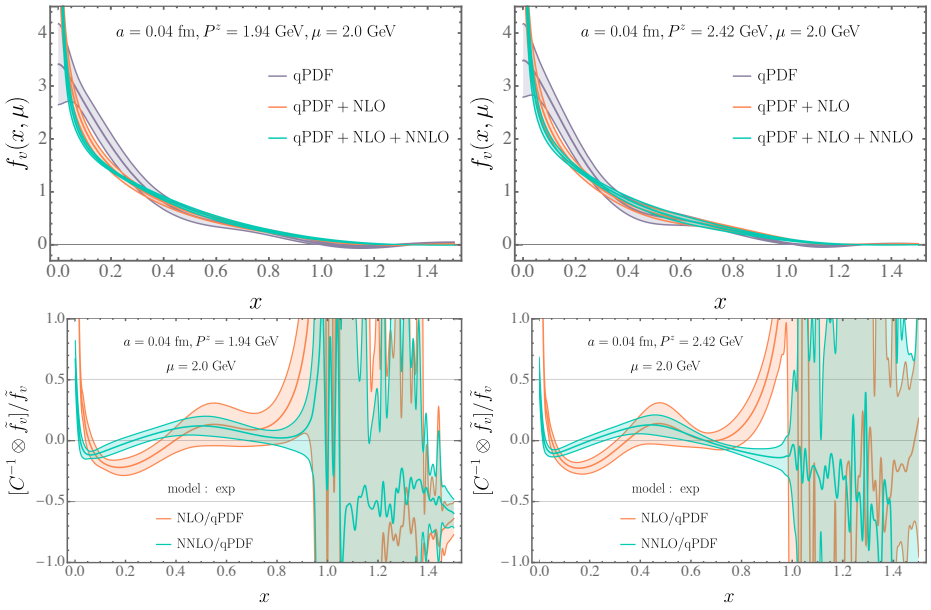


**Figure 4:** Upper panels: the qPDF (or LO PDF), and the ones after NLO and NNLO matching corrections are shown for comparison. Lower panels: the ratio of NLO and NNLO corrections to the qPDF.

corrections and power corrections. Firstly, it has been observed in Fig. 1 that the renormalized matrix elements of 300 MeV pion from different lattice spacings show little discretization effect as overlaping with each other. In addition, we have another calculation of $a = 0.076$ fm ensemble with 140 MeV pion. In Fig. 3, we show the valence quark distribution $f_v(x,\mu)$ after the NNLO LaMET matching from different lattices but similar momentum. As one can see, when boosted momenta as large as $P_z \gtrsim 1.5$ GeV, the pion mass dependence is little and smaller than the statistical errors. Therefore, in our calculations with fine lattice spacings and high boosted momentum, the lattice artifacts are small.

Then we consider the convergence of the perturbative matching. In the upper panel of Fig. 4, we show the qPDF (or LO PDF), and corresponding PDF after NLO and NNLO matching corrections

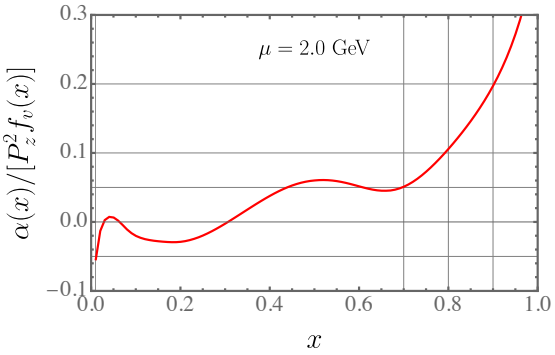


**Figure 5:** The ratio of power corrections $\alpha(x)/P_z^2$ over $f_v(x)$ obtained from our largest momentum $P_z = 2.42$ GeV are shown.

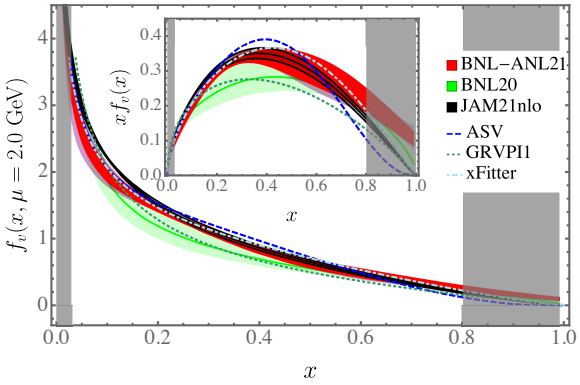


**Figure 6:** The pion valence quark PDF $f_v(x)$ from NNLO LaMET matching is shown, where the darker red band is the statistical errors while the lighter red band is the systematic errors from scale variation. For comparison, we also show the results from global analysis [40–43] and lattice determination from BNL20 [17].

for two large momentum. The the ratio of NLO and NNLO corrections to the qPDF $[C^{-1} \otimes \tilde{f}_v]/\tilde{f}_v$ are shown in the lower panels. As one can see, in the middle region of $x$ the perturbative corrections are small compared to the LO qPDF and get smaller from NLO to NNLO. This observation suggests the good convergence of the perturbative matching. Targeting a precision of 5% of perturbation uncertainty, we require the NNNLO correction $O(\alpha_s^3)$ at $\mu = 2.0$ GeV smaller than 5%, which can be propagated to the NLO and NNLO corrections smaller than $(5\%)^{1/3} = 37\%$ and $(5\%)^{2/3} = 14\%$ assuming the perturbation series grows geometrically. This requirement excludes the regions $x < 0.03$ and $x > 0.88$ for PDF obtained from our largest momentum. We also consider the scale variation by extracting the PDF at $\mu$ from 1.4 to 2.8 GeV and evolving them to $\mu = 2.0$ GeV using DGLAP evolution.

As mentioned in Sec. 3, the LaMET factorization has power corrections driven by $P_z$ at the end point region of $x$ as $O(1/(xP_z)^2)$ and $O(1/((1-x)P^z)^2]$ [32]. To estimate the power corrections, we parametrize the $P_z$ dependence at each $x$ as $f_v(x) + \alpha(x)/P_z^2$ using $f_v(x)$ obtained from $P^z = \{1.45, 1.72, 1.94, 2.15, 2.42\}$ GeV. We show the ratio of power corrections $\alpha(x)/P_z^2$ over $f_v(x)$ obtained from our largest momentum $P_z = 2.42$ GeV in Fig. 5, in which $\alpha(x)/[P_z^2 f_v(x)] \lesssim 0.1$

corresponding to $0.01 < x < 0.80$ and $\alpha(x)/[P_z^2 f_v(x)] \lesssim 0.05$ corresponding to $0.01 < x < 0.70$.

We show our final results in Fig. 6 coming from our largest momentum $P_z = 2.42$ GeV of $a = 0.04$ fm and $z_S = 0.24$ fm at factorization scale $\mu = 2.0$ GeV, with the darker red band being the statistical errors and the lighter band being the systematical errors from scale variation. By summing over the statistical errors and all kind systematic errors discussed above, we determine the pion valence PDF at $0.03 \lesssim x \lesssim 0.80$ with fully controlled 5–20% uncertainties. Results from global analysis are also shown for comparison, where better agreement can be observed with the most recent two from JAM21nlo [41] and xFitter [40] for $0.2 < x < 0.6$ then the older ones. We also compare with the determination from short distance factorization of the lattice data using certain models (BNL20) [17]. Though we overlap each other, the result in this work have smaller error bars in middle $x$ and the BNL20 has uncontrolled model bias.

In this work, we present the $x$ dependent pion valence PDF from lattice calculations with LaMET matching. We calculate the pion bare matrix elements with large momentum from multiple lattices, and renormalize them using most advanced hybrid scheme. We considered statistical errors and possible systematic errors, and provide reliable prediction of $x$ dependence with quantified uncertainties. It is encouraging to see our determination from pure lattice calculations have good agreement with the most recent global analysis. The procedure in this work can be applied to other kinds of PDFs for a reliable prediction.

## Acknowledgments

This material is based upon work supported by: (i) The U.S. Department of Energy, Office of Science, Office of Nuclear Physics through Contract No. DE-SC0012704 and No. DE-AC02-06CH11357; (ii) The U.S. Department of Energy, Office of Science, Office of Nuclear Physics and Office of Advanced Scientific Computing Research within the framework of Scientific Discovery through Advance Computing (SciDAC) award Computing the Properties of Matter with Leadership Computing Resources; (iii) The U.S. Department of Energy, Office of Science, Office of Nuclear Physics, within the framework of the TMD Topical Collaboration. (iv) XG is partially supported by the NSFC under the grant number 11775096 and the Guangdong Major Project of Basic and Applied Basic Research No. 2020B0301030008. (v) SS is supported by the National Science Foundation under CAREER Award PHY-1847893 and by the RHIC Physics Fellow Program of the RIKEN BNL Research Center.. (vi) This research used awards of computer time provided by the INCITE and ALCC programs at Oak Ridge Leadership Computing Facility, a DOE Office of Science User Facility operated under Contract No. DE-AC05-00OR22725. (vii) Computations for this work were carried out in part on facilities of the USQCD Collaboration, which are funded by the Office of Science of the U.S. Department of Energy. viii) YZ is partially supported by an LDRD initiative at Argonne National Laboratory under Project No. 2020-0020.

## References

[1] A. Accardi *et al.*, Eur. Phys. J. A **52**, 268 (2016), arXiv:1212.1701 [nucl-ex] .

[2] R. Abdul Khalek *et al.*, (2021), arXiv:2103.05419 [physics.ins-det] .

[3] A. C. Aguilar *et al.*, Eur. Phys. J. A **55**, 190 (2019), arXiv:1907.08218 [nucl-ex] .

[4] X. Ji, Phys. Rev. Lett. **110**, 262002 (2013), arXiv:1305.1539 [hep-ph] .

[5] X. Ji, Sci. China Phys. Mech. Astron. **57**, 1407 (2014), arXiv:1404.6680 [hep-ph] .

[6] X. Ji, Y.-S. Liu, Y. Liu, J.-H. Zhang, and Y. Zhao, Rev. Mod. Phys. **93**, 035005 (2021), arXiv:2004.03543 [hep-ph] .

[7] M. Constantinou *et al.*, Prog. Part. Nucl. Phys. **121**, 103908 (2021), arXiv:2006.08636 [hep-ph] .

[8] M. Constantinou *et al.*, (2022), arXiv:2202.07193 [hep-lat] .

[9] Z. Fan, X. Gao, R. Li, H.-W. Lin, N. Karthik, S. Mukherjee, P. Petreczky, S. Syritsyn, Y.-B. Yang, and R. Zhang, Phys. Rev. D **102**, 074504 (2020), arXiv:2005.12015 [hep-lat] .

[10] Z.-Y. Fan, Y.-B. Yang, A. Anthony, H.-W. Lin, and K.-F. Liu, Phys. Rev. Lett. **121**, 242001 (2018), arXiv:1808.02077 [hep-lat] .

[11] Z. Fan, R. Zhang, and H.-W. Lin, Int. J. Mod. Phys. A **36**, 2150080 (2021), arXiv:2007.16113 [hep-lat] .

[12] T. Khan *et al.* (HadStruc), Phys. Rev. D **104**, 094516 (2021), arXiv:2107.08960 [hep-lat] .

[13] X. Gao, A. D. Hanlon, N. Karthik, S. Mukherjee, P. Petreczky, P. Scior, S. Shi, S. Syritsyn, Y. Zhao, and K. Zhou, (2022), arXiv:2208.02297 [hep-lat] .

[14] X. Gao, K. Lee, S. Mukherjee, C. Shugert, and Y. Zhao, Phys. Rev. D **103**, 094504 (2021), arXiv:2102.01101 [hep-ph] .

[15] Z. Fan and H.-W. Lin, Phys. Lett. B **823**, 136778 (2021), arXiv:2104.06372 [hep-lat] .

[16] X. Gao, N. Karthik, S. Mukherjee, P. Petreczky, S. Syritsyn, and Y. Zhao, Phys. Rev. D **103**, 094510 (2021), arXiv:2101.11632 [hep-lat] .

[17] X. Gao, L. Jin, C. Kallidonis, N. Karthik, S. Mukherjee, P. Petreczky, C. Shugert, S. Syritsyn, and Y. Zhao, Phys. Rev. D **102**, 094513 (2020), arXiv:2007.06590 [hep-lat] .

[18] J.-H. Zhang, J.-W. Chen, L. Jin, H.-W. Lin, A. Schäfer, and Y. Zhao, Phys. Rev. D **100**, 034505 (2019), arXiv:1804.01483 [hep-lat] .

[19] T. Izubuchi, L. Jin, C. Kallidonis, N. Karthik, S. Mukherjee, P. Petreczky, C. Shugert, and S. Syritsyn, Phys. Rev. D **100**, 034516 (2019), arXiv:1905.06349 [hep-lat] .

[20] R. S. Sufian, C. Egerer, J. Karpie, R. G. Edwards, B. Joó, Y.-Q. Ma, K. Orginos, J.-W. Qiu, and D. G. Richards, Phys. Rev. D **102**, 054508 (2020), arXiv:2001.04960 [hep-lat] .

[21] R. S. Sufian, J. Karpie, C. Egerer, K. Orginos, J.-W. Qiu, and D. G. Richards, Phys. Rev. D **99**, 074507 (2019), arXiv:1901.03921 [hep-lat] .

[22] P. C. Barry *et al.* (Jefferson Lab Angular Momentum (JAM), HadStruc), Phys. Rev. D **105**, 114051 (2022), arXiv:2204.00543 [hep-ph] .

[23] J. Karpie, K. Orginos, and S. Zafeiropoulos, JHEP **11**, 178 (2018), arXiv:1807.10933 [hep-lat] .

[24] J. Karpie, K. Orginos, A. Radyushkin, and S. Zafeiropoulos (HadStruc), JHEP **11**, 024 (2021), arXiv:2105.13313 [hep-lat] .

[25] C. Shugert, X. Gao, T. Izubichi, L. Jin, C. Kallidonis, N. Karthik, S. Mukherjee, P. Petreczky, S. Syritsyn, and Y. Zhao, in *37th International Symposium on Lattice Field Theory* (2020) arXiv:2001.11650 [hep-lat] .

[26] A. Bazavov *et al.* (HotQCD), Phys. Rev. D **90**, 094503 (2014), arXiv:1407.6387 [hep-lat] .

[27] E. Follana, Q. Mason, C. Davies, K. Hornbostel, G. P. Lepage, J. Shigemitsu, H. Trottier, and K. Wong (HPQCD, UKQCD), Phys. Rev. D **75**, 054502 (2007), arXiv:hep-lat/0610092 .

[28] X. Ji, J.-H. Zhang, and Y. Zhao, Phys. Rev. Lett. **120**, 112001 (2018), arXiv:1706.08962 [hep-ph] .

[29] T. Ishikawa, Y.-Q. Ma, J.-W. Qiu, and S. Yoshida, Phys. Rev. D **96**, 094019 (2017), arXiv:1707.03107 [hep-ph] .

[30] J. Green, K. Jansen, and F. Steffens, Phys. Rev. Lett. **121**, 022004 (2018), arXiv:1707.07152 [hep-lat] .

[31] C. Bauer, G. S. Bali, and A. Pineda, Phys. Rev. Lett. **108**, 242002 (2012), arXiv:1111.3946 [hep-ph] .

[32] X. Ji, Y. Liu, A. Schäfer, W. Wang, Y.-B. Yang, J.-H. Zhang, and Y. Zhao, Nucl. Phys. B **964**, 115311 (2021), arXiv:2008.03886 [hep-ph] .

[33] X. Gao, A. D. Hanlon, S. Mukherjee, P. Petreczky, P. Scior, S. Syritsyn, and Y. Zhao, Phys. Rev. Lett. **128**, 142003 (2022), arXiv:2112.02208 [hep-lat] .

[34] T. Izubuchi, X. Ji, L. Jin, I. W. Stewart, and Y. Zhao, Phys. Rev. D **98**, 056004 (2018), arXiv:1801.03917 [hep-ph] .

[35] L.-B. Chen, W. Wang, and R. Zhu, Phys. Rev. Lett. **126**, 072002 (2021), arXiv:2006.14825 [hep-ph] .

[36] Z.-Y. Li, Y.-Q. Ma, and J.-W. Qiu, Phys. Rev. Lett. **126**, 072001 (2021), arXiv:2006.12370 [hep-ph] .

[37] V. M. Braun, A. Vladimirov, and J.-H. Zhang, Phys. Rev. D **99**, 014013 (2019), arXiv:1810.00048 [hep-ph] .

[38] X. Xiong, X. Ji, J.-H. Zhang, and Y. Zhao, Phys. Rev. D **90**, 014051 (2014), arXiv:1310.7471 [hep-ph] .

[39] Y.-Q. Ma and J.-W. Qiu, Phys. Rev. D **98**, 074021 (2018), arXiv:1404.6860 [hep-ph] .

[40] I. Novikov *et al.*, Phys. Rev. D **102**, 014040 (2020), arXiv:2002.02902 [hep-ph] .

[41] P. C. Barry, C.-R. Ji, N. Sato, and W. Melnitchouk (Jefferson Lab Angular Momentum (JAM)), Phys. Rev. Lett. **127**, 232001 (2021), arXiv:2108.05822 [hep-ph] .

[42] M. Gluck, E. Reya, and A. Vogt, Z. Phys. C **53**, 651 (1992).

[43] M. Aicher, A. Schafer, and W. Vogelsang, Phys. Rev. Lett. **105**, 252003 (2010), arXiv:1009.2481 [hep-ph] .